American Mineralogist, Volume 67, pages 1144–1154, 1982

Techniques for using iron crucibles in experimental igneous petrology

CARL R. THORNBER AND J. STEPHEN HUEBNER

U.S. Geological Survey
959 National Center
Reston, Virginia 22092

Abstract

Some iron metal used to fabricate crucibles contains impurities comprising manganese, titanium and other elements. Under closed-system conditions these impurities impose an f_{O_2} that can differ from that of a silicate charge in equilibrium with pure metallic iron. Equilibration of the impurities in the crucible with the charge can reduce the iron oxide component of the charge and contaminate it with manganese and titanium. Pretreatment of impure iron crucibles in a CO_2–CO atmosphere at 1050°C, under conditions slightly more reducing than Fe–$Fe_{1-x}O$, minimizes undesirable changes in the bulk composition of the charge.

Introduction

Bowen and Schairer (1932), in their study of the iron-oxide–SiO_2 system, pioneered the use of iron crucibles to "control and define" iron oxide in its ferrous state at high temperature. However, Bowen and coworkers, and others using metallic iron to contain iron oxide-bearing materials, found apparently unpredictable variations in the ferrous-iron content of the run products. Iron-bearing silicate charges in iron crucibles open to an atmosphere of purified nitrogen are gradually oxidized, as reflected by the progressive oxidation of the metallic iron capsule and a steady increase in ferrous iron content of the charge with time. This change was ascribed to the small but significant proportion of oxygen present in the "inert" gas and was avoided by keeping run times to "not more than fifteen minutes" (Bowen and Schairer, 1932, p. 179; 1935; Bowen *et al.*, 1933), a run duration supposedly sufficient for achievement of crystal/melt equilibrium in their system, but one which is probably not adequate for all systems. In systems open to an atmosphere of mixtures of CO_2 and H_2 or CO_2 and CO gases, accumulation or depletion of ferrous iron in the charge is the result of either oxidation of metallic iron in contact with the charge or reduction of iron oxide within the charge. The extent of change is primarily controlled by run duration and the oxygen fugacity (f_{O_2}) of the gas mixture (*e.g.*, Roeder, 1974, Fig. 1). An additional problem with the open-system technique is volatilization and loss of alkalis from the charge, resulting in changes in bulk composition which affect changes in the oxidation state of iron (Thornber *et al.* 1980).

Experimental research on the petrogenesis of lunar samples necessitated devising methods to contain silicate melts at low f_{O_2} that are in equilibrium with metallic iron (disseminated throughout some lunar rocks) while maintaining the bulk composition of the charge for a time sufficient to reach equilibrium—a period of hours to days or even weeks. Toward this end, Muan and Schairer (1970) revived a method, originally explored (and discarded) by Bowen and Schairer (1932), of sealing charges in iron crucibles, which in turn are sealed in evacuated silica-glass tubes. Muan and Schairer reported significant ferrous-iron gain in charges and attributed it to a reaction between the metal crucible and ferric iron in the starting mixture.

Subsequent experimental work on natural and synthetic lunar materials, in similar closed systems, has been sporadically plagued by analogous problems of iron gain or loss. The implications of such undesired, perhaps unrecognized, bulk-composition changes and explanations for their cause are discussed by Kesson (1975) and Walker *et al.* (1975, 1976) and are summarized by O'Hara and Humphries (1977). Because of the successful use of ultra-high-purity iron crucibles (Johnson-Mathey Grade 1, 99.998% Fe)[1] by Kesson (1975), Walker *et*

---

[1] Any use of trade names in this publication is for descriptive purposes only and does not constitute endorsement by the U.S. Geological Survey.

0003–004X/82/1112–1144$02.00

al. (1977), Longhi *et al.* (1974), and Green *et al.* (1975), recent workers have generally assumed that less pure iron crucible material, such as "ingot" grade iron (Grove *et al.*, 1973; Walker *et al.*, 1972) or electromagnet-grade iron (Muan and Schairer, 1970; Thornber and Huebner, 1980), may impart undesirable changes in the bulk composition of the charge.

Problems of ferrous-iron loss encountered by the present authors in their experimental study of the thermal history of lunar fragment-laden basalt 77115 (Thornber and Huebner, 1980) prompted a systematic investigation of the use of iron crucibles in closed systems. We wanted to understand the nature of impurities in crucible materials, their role in governing redox equilibria, and the effect of the impurities upon the bulk composition of the charges. Despite the obvious disadvantages of using impure iron crucibles, this material is, by virtue of being less expensive, more expendable. Polished thin sections can be cut through the crucible without concern for its reclamation, allowing observation of an entire cross-section through the charge and thus a more complete evaluation of its chemical and textural variability. In particular, observation of the crucible-charge interface textures is often critical for the recognition of crystal nucleation on crucible walls. For this reason, we sought methods of using relatively impure iron crucibles by minimizing or eliminating undesirable effects of crucible-charge interaction.

Characterization of iron metals investigated

Previous investigators considered the relevant impurities in iron capsules to be carbon (Biggar *et al.*, 1974; Longhi *et al.*, 1974) and phosphorus (Walker *et al.*, 1976, 1977). We also initially considered the possibility that sulfur, arsenic and hydrogen (the last occluded during refining and manufacturing of the iron rod stock) might be undesirable impurities. However, typical mill analyses of impure iron do not report hydrogen and show carbon, arsenic, phosphorus, and sulfur at levels too low to account for the observed iron gain or loss.

Petrographic examination of iron from different sources reveals characteristics that might be used to select the most suitable iron for different experiments. We can distinguish different lots of impure iron on the basis of their inclusions (Figs. 1a, b, and Table 1). For example, different lots of electromagnet-grade iron contain at least 1 volume percent of impurities in the form of 1 to ~10 micrometer medium- and dark-grey blebs, yellow prisms and minor plum-pink and tan-colored inclusions. Qualitative chemical analysis by energy-dispersive electron microprobe and scanning-electron-microscope techniques reveals that the inclusions contain various combinations of manganese, titanium, iron, nickel, chromium, aluminum, silicon and sulfur (Table 1). The yellow prismatic phase has the color and morphological characteristics of titanous oxide (TiO). Materials Research Corp. MARZ grade and Johnson–Mathey specpure foil do not show any inclusions or precipitates when examined with a petrographic microscope at 800× magnification.

The bulk chemistry of some lots of iron metal is not known. Clearly, however, at least some analyses supplied by manufacturers fail to report potential reducing agents such as hydrogen, and show titanium and manganese values (Table 2) that are too low to account for the observed inclusions (much less any additional titanium and manganese alloyed with the iron). Analyses of high-purity iron show negligible amounts of manganese and titanium (Table 2), consistent with the absence of inclusions (Table 1) in iron.

Experimental methods

Our experiments used crucibles of iron (Corey Steel Corp. lot #92474, Armco electromagnet-grade and Materials Research Corp. lot #26/1926 VP-grade, Table 2) and a sintered glass having the composition of lunar basalt 77115 (Thornber and Huebner, 1980). The crucibles were 0.250 inch in diameter and 0.30 inch long. The inner bore was 0.205 inch in diameter and finished with a conical bottom, giving a maximum depth of 0.26 inch. A typical capsule weighed ~1 gm. The crucibles were machined and stored in low sulfur oil, a procedure proven effective by Walker *et al.* (1977), cleaned in spectrographic grade N–Heptane or Freon, and then stored in a vacuum desiccator.

The sintered glass was prepared by thrice fusing at ~1300°C (in air) a manganese-free reagent-grade oxide-and-carbonate mix, in a platinum crucible pretreated with the mix under similar conditions. To assure homogeneity, the oxidized glass was crushed and ground in reagent-grade isopropyl alcohol before each remelting. The composition of the glass measured after the third fusion is presented in Table 3. The oxidized glass was then placed in a presaturated $Ag_{70}Pd_{30}$ alloy container and reduced at 1050°C and 1 bar pressure in a CO_2 and H_2 gas mixture with an f_{O_2} of $10^{-13.5}$ bar. Particular care

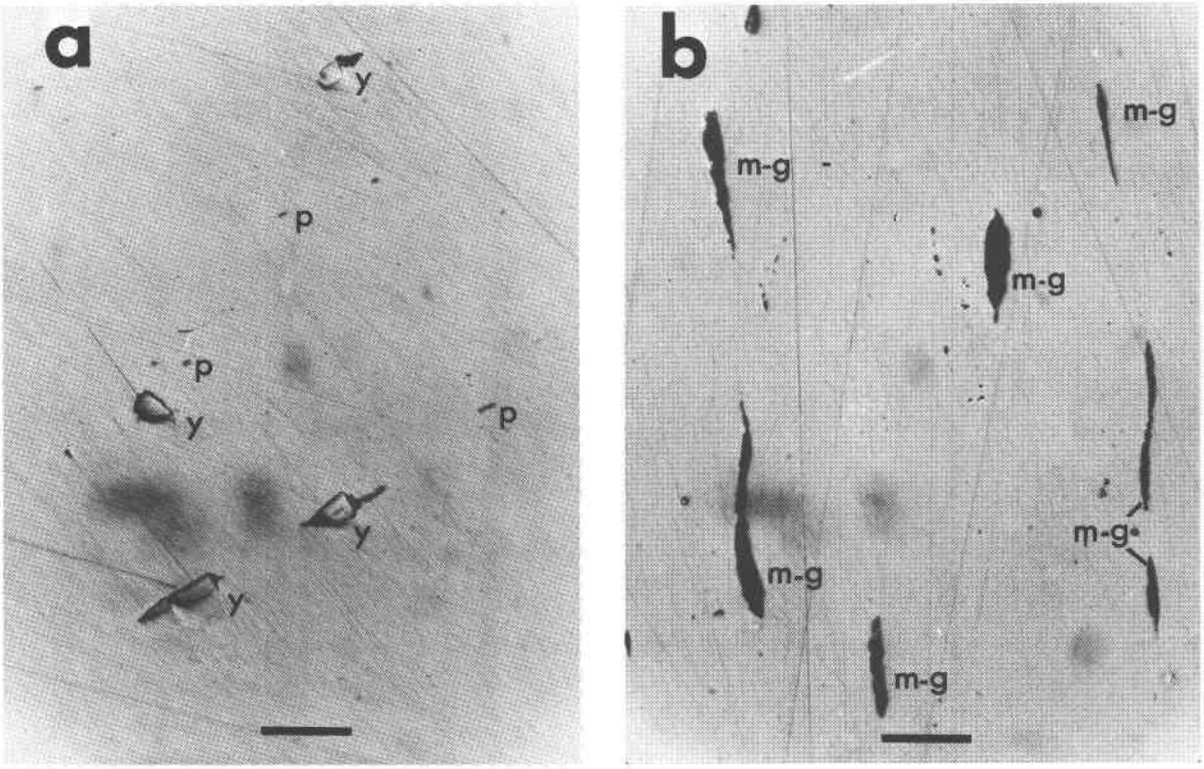

Fig. 1. Reflected-light photomicrographs (oil immersion) showing inclusions in different lots of Armco electromagnet-grade iron; (a) yellow prisms (y) and plum-colored blebs (p) in Corey Steel Corp. lot #92474, (b) medium-grey elongate blebs m–g in Lipin/Muan Rod. Bar scale in each photograph represents 25 μm.

was taken to preserve the composition of the reduced and sintered glass by quenching it in liquid nitrogen, then storing it in a vacuum desiccator. The sintered product was tested with a magnet and characterized by X-ray diffraction and optical techniques, all of which showed that it contained a negligible amount of metallic iron. The sintered starting material was ground in alcohol, dried in air and loaded into iron crucibles. The same batch of reduced starting material was used in all experiments reported in this investigation.

Hydrogen treatment of crucibles was accomplished by heating them at ~825°C in a stream of hydrogen which flowed through a silica tube in a horizontal furnace. Crucibles in this assembly were brought up to temperature (~1/2 hour), heated for 1 hour, and then cooled to room temperature (~1/2 hour) before removal. In the presence of the hydrogen stream, iron, manganese, and titanium are all stable as metals. Several such capsules were baked in a vacuum before being filled with silicate charge. Our intention in including this extra step was to determine whether or not H_2 could be removed from α–iron (at 800°C) or γ–iron (at 1100°C).

Some crucibles were annealed at 1050°C and 1 bar in a flowing gas mixture of CO_2 and H_2 *or* CO_2 and CO. The latter mixture was used when a hydrogen-free atmosphere was needed. Ideally, the mixing ratios 9–21 for CO_2–H_2 or 7–23 for CO_2–CO define the same furnace f_{O_2} values ($10^{-14.6}$ bar, compared with $10^{-14.0}$ for Fe–$Fe_{1-x}O$). Practically, the temperature may have been too low for the achievement of furnace-gas equilibrium (Huebner, 1975); if so, the prevailing f_{O_2} would have been more reducing. Nevertheless, at all f_{O_2} values believed encountered, iron metal, MnO, and TiO_2 are stable phases. The crucibles were quenched in a manner that did *not* cause oxidation or otherwise alter their composition. Drop-quenching risks contamination with carbon, a stable and ever-present phase in the cool, upstream portion of the flowing CO_2–CO gas mixture. The best procedure proved to be rapid removal from the top (downstream) end of the furnace and movement through a N_2-rich atmo-

Table 1. Description and qualitative analyses of inclusions in iron-crucible materials

Iron Material	Inclusion Type					
	Yellow (prisms)	Plum (blebs)	Tan (blebs)	Medium-grey (blebs)	Medium-grey (elongate blebs)	Dark-grey (blebs)
Armco[†] rod (Corey Steel lot #92474)	X	X				
Armco[†] rod (Corey Steel lot #91913)	X	X				
Armco[†] rod (Corey Steel lot #91368)	X					
Batten crucibles 0.25" diam.	X	X				X
Batten crucibles 0.10" diam.				X		
Armco[†] rod (Lipin/ Muan)			X		X	X
Armco[†] crucible Roeder (1974)			X	X		X
MRC VP rod (lot #26/1926)	trace					
MRC Marz rod (lot #26/2226)	no inclusions observed					
Johnson-Mathey (specpure foil)	no inclusions observed					
Armco[†] rod 92474:						
CO_2/H_2 treated	X	X		X		X
CO_2/CO treated	X	X		X		X
H_2 treated	no inclusions observed					
Armco[†] rod (Lipin/Muan) H_2 treated	no inclusions observed					
Elements present in inclusion						
Al						X
Si						X
S		X	X			X
Ca						X
Ti	X	X				
Cr					X	X
Mn			X	X	X	X
Fe*		X	X	X	X	X
Ni			X			X

[†] *Electromagnet-grade iron*

[*] *Fe detected may be due to surrounding iron host.*

sphere (eminating from the dewer with liquid nitrogen) and into the liquid nitrogen to minimize contact with air.

All capsules were filled with sintered glass such that the crucible-to-sample weight-ratio was 16.0± 0.5. After the capsules were loaded, their lids were loosely fitted, and charge and crucible were heated (825°C) in a vacuum for 10 minutes to dry the charge and remove any hydrocarbons introduced during charge or crucible preparation. Iron sponge, previ-

Table 2. Chemical analyses of iron crucible materials (ppm)

	Armco electro-[1] magnetic iron	Batten[2] crucibles	MRC VP[3]	MRC Marz[4]
C	100	150	18.0	12.0
Si	NA	30	50.0	<0.10
P	80	50	ND	0.70
Al	500	NA	60.0	<0.10
S	200	250	40.0	2.60
Ti	700	NA	<10.0	1.40
Cr	NA	NA	30.0	1.60
Mn	800	280	NA	NA
Other ( )	NA	NA	165 (max)	7.57 (max)
Fe (wt%)	99.762	99.924	99.997 (min)	99.997 (min)

[1] "Typical mill" analysis Cory Steel Company (emission spectrographic only)

[2] Representative analysis supplied by C.A. Batten & Sons, Inc.

[3] Materials Research Corporation lot #26/1926 conductometric (carbon); Leco method (gases); emission spectrographic (others)

[4] Materials Research Corporation lot #26/2226 conductometric (carbon); Leco method (gases); mass spectrographic (others)

NA, not analysed; ND, not detected

ously sintered in hydrogen, was placed between the crucible and the pump, positioned at a slightly lower temperature (~800°C). The porous sponge captures oxygen (and possibly oil vapor?) that backstreams from the pump. Next, tapered lids were fitted by friction into crucibles using a punch, the loaded crucibles were enclosed in evacuated silica tubes (0.045 in. wall thickness), and the run assemblies were heated above the charge's liquidus at 1250°C. Finally, the tubes were drop-quenched into water and a polished thin section enclosing the axis of the crucible and charge was prepared. Controlled variables in the experiments were the purity of iron crucible material (either electromagnet-grade iron or VP iron), the method by which crucibles were pretreated, and the run duration. Major- and minor-element compositions of the product glasses were determined by electron-microprobe techniques using an ARL-EMX microprobe, combined EDS and WDS techniques (Wiggins and Huebner, 1981) and glass standard VG-A99 (Jarosewich *et al.*, 1979).

Experimental results: pretreatment of iron

The treatment of electromagnet-grade iron at high temperatures in gas mixtures of CO_2–H_2 and CO_2–CO (at f_{O_2} values that are ideally slightly below those of the assemblage Fe–$Fe_{1-x}O$ gas) results in the development of the manganese–titanium rich phases (Fig. 2); conversely, reduction of the capsule material in hydrogen gas diminishes the occurrence of inclusions as they are reduced and alloy with the metallic iron. This result can be explained by considering the values of f_{O_2} used in the capsule pretreatment. At relatively high f_{O_2} the manganese and titanium, originally present in iron-rich alloy, are oxidized and form included precipitates. At the extremely low f_{O_2} values characteristic of the hydrogen-rich atmosphere, the metallic state is stable and both manganese and titanium tend to alloy with the iron. We have no evidence that the pretreatment changes the *bulk* composition with respect to manganese and titanium; rather, these elements are simply redistributed among the phases present.

Oxidation halos formed when impure crucibles were annealed in the CO_2–H_2 or CO_2–CO gas mixtures. On oxidation, the prismatic, yellow TiO precipitates are altered to grey manganese–titanium oxide. The width of the halo is defined as the depth of this oxidation from the crucible surface, and is distinctly different in capsules treated in CO_2–H_2 and CO_2–CO gas mixtures, but at the same nominal values of oxygen fugacity and temperatures. In crucibles treated in CO_2–H_2 for 143 hours, rind width is ~200 microns, yet CO_2–CO treatments for

Table 3. Composition of glass starting material (fused three times in air)

	Average of 10 analyses	
Oxide	Weight %	Standard deviation
SiO_2	44.0	0.69
TiO_2	2.8	0.13
Al_2O_3	17.0	0.31
FeO*	9.5	0.29
O_2**	1.06	
MnO	0.02	0.047
MgO	10.6	0.41
CaO	12.2	0.18
Na_2O	1.75	0.286
K_2O	0.08	0.066
Total	99.01	

* All iron recalculated as FeO

** "Excess" oxygen assuming all iron is ferric

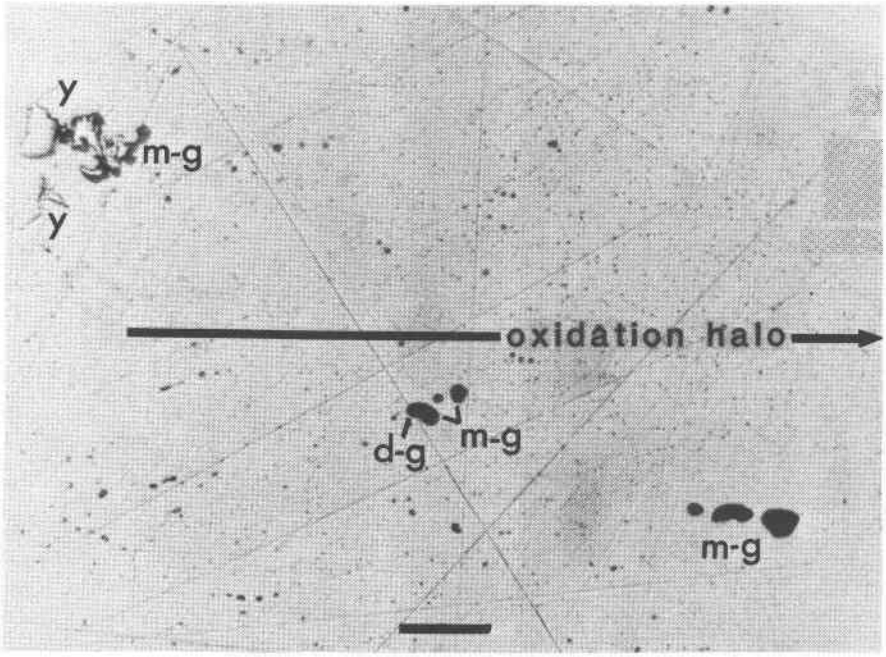

Fig. 2. Reflected-light photomicrograph (oil immersion) showing oxidation halo in CO_2–CO-treated electromagnet-grade iron crucible. Arrow points toward edge of crucible. Note medium-grey oxidation rim around yellow prisms (y) and development of medium and dark-grey blebs (m–g and d–g). Bar scale represents 25 μm.

only 96 hours resulted in a rind which is ~270 microns wide. This difference could be due to the preferential permeation of hydrogen from the CO_2–H_2 furnance gas deep into the metal, where it would tend to retard oxidation. (As we will see later, this conclusion is supported by the relative difference in iron loss with time in runs using CO_2–H_2 pretreated crucibles as compared with similar experiments in CO_2–CO treated crucibles.)

The effect of H_2 treatment on impure iron crucibles is most readily observed in the electromagnet-grade material which contains abundant grey manganiferous inclusions (Lipin/Muan Rod), presumably a manganous oxide. Exposure to the H_2 atmosphere at high temperature results in development of numerous vugs, some of which surround remnant oxides at the outer extremities of the rod.

In contrast to the behavior of manganese and titanium, crucible pretreatment appears to change the bulk volatile content of the metal. Treatment at low f_{O_2} effectively removes oxide tarnish, leaving the crucibles shiny and bright. We also found that annealing in hydrogen reduces the carbon content of electromagnet-grade iron from ~100 ppm (Table 2) to ≤30 ppm (the detection limit using a U.S. Geological Survey carbon analyzer). Presumably carbon is carried off as CH_4 gas.

Experimental results: equilibration with silicate melt

All electromagnet-grade crucibles treated in hydrogen gas and run with silicate melt according to the procedure described above caused loss of iron from the glass (Table 4; Figure 3). The degree of iron loss increased with time of run and exceeded 79% in 24 hours. The progressive reduction of FeO in the silicate charges is reflected by increased abundance of coarse blebs of metallic iron in the melt as well as the nature and abundance of inclusions observed within the crucible. An oxidation front is developed progressively inward from the surface to the interior of the crucible in these runs, and is characterized by manganese and titanium oxide blebs which are more abundant at the crucible/charge interface and grade inward toward the interior of the crucible which is "cleaner" and contains occasional yellow prisms in a metallic host (Fig. 4). The progressive nature of this oxidation front is clearly indicated by the decrease in abundance of the oxide inclusions as one passes from the crucible-melt interface toward the interior of the iron metal, and by an inner transition zone where relic yellow crystals are rimmed by grey Mn–Ti oxide. This oxidation halo thickens with time while

Table 4. Run summary

Run number	Crucible* material	Crucible pretreatment			Vacuum heating		Run data		Results
		atmosphere	temp(°C)	time(hrs)	before loading	after loading	temp (°C)	time (hrs)	wt% Iron as FeO
46	EM	untreated			no	yes	1250	24	1.0
22	EM	untreated			no	yes	1252	151	2.1
	EM								
10	EM	H_2	825	2	no	yes	1250	8	4.8
6	EM	H_2	825	2	no	yes	1250	24	2.0
7	EM	H_2	825	2	no	yes	1250	48	1.3
8	EM	H_2	825	2	no	yes	1250	142	0.7
14	EM	H_2	825	2	yes	yes	1250	23.5	1.8
13	EM	H_2	825	2	yes	yes	1253	48	4.8
15	EM	H_2	825	2	yes	yes	1250	120.5	2.1
34	EM	H_2	825	2	1100°C/ 1/4 hr	yes	1250	48	1.3
36	EM	H_2	825	2	1100°C/ 1 hr	yes	1250	48	1.6
5	EM	CO_2-H_2	1050	163	no	yes	1252	24	6.7
4	EM	CO_2-H_2	1050	160	no	yes	1251	48	5.3
3	EM	CO_2-H_2	1050	160	no	yes	1250	143	3.2
17	EM	CO_2-CO	1050	96	no	yes	1250	48	10.7
42	EM	CO_2-CO	1100	48	no	yes	1250	68	10.7
18	EM	CO_2-CO	1050	96	no	yes	1250	120	9.3
43	EM	CO_2-CO	1100	48	no	yes	1250	122.5	9.5
19	VP	untreated			no	yes	1252	24	9.4
20	VP	untreated			no	yes	1252	77	10.3
21	VP	untreated			no	yes	1252	151	10.0
41	VP	H_2	825	2	no	yes	1250	24	9.7
38	VP	H_2	825	2	no	yes	1250	162.5	11.4
44	VP	H_2	825	2	no	no	1252	96	10.3
39	VP	CO_2-H_2	1100	116	no	yes	1250	24	11.4
40	VP	CO_2-H_2	1100	116	no	yes	1250	92	11.9

*EM: *Cory Steel lot #92474, Armco electromagnet-grade iron*

*VP: *Materials Research Corporation lot #26/1926, VP-grade iron*

the FeO content of the melt decreases (Fig. 3). We believe that the oxidation of manganese (and perhaps titanium) alloyed in the iron, and the conversion of reduced titanium oxide to higher oxides, can reduce FeO initially present in the silicate melt.

Iron loss from melts contained in hydrogen-treated electromagnet-grade crucibles, annealed in a vacuum before being loaded, is sporadic and comparable to that observed in runs using untreated electromagnet-grade crucibles (Table 4). Thus, hydrogen and vacuum heat-treatment of impure iron, despite removing carbon, is unsatisfactory. There were no inclusions observed in crucibles of VP iron pretreated in hydrogen or in a CO_2–H_2 gas mixture, and no substantial changes in FeO concentration were observed in runs using either treated or untreated high-purity iron containers. Furthermore, no inclusions formed in the crucibles during these runs.

Electron-microprobe analyses of charges run in impure crucibles demonstrate that transition metal impurities diffuse from the capsule and into the silicate melt. The concentrations of MnO and TiO_2 within the charge are shown to increase with time (Fig. 5), indicating movement of manganese and titanium from the crucible and into the charge. This observation, in conjunction with that of an increased abundance of oxide impurities at the crucible-charge interface, is suggestive of mutual diffusion of manganese and titanium into the charge and

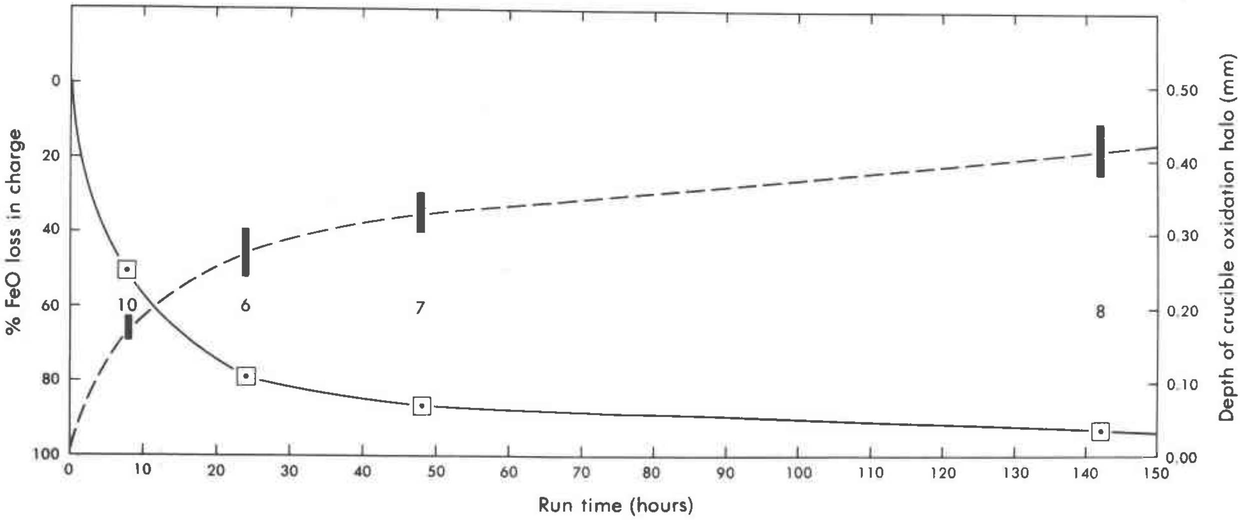

Fig. 3. Percent FeO loss in charge (solid line/left ordinate) and depth of crucible oxidation halo (dashed line/right ordinate) *vs.* time in charges run in H_2-treated electromagnet-grade iron crucibles. Length of bars represents total variation of 10 depth measurements. Run numbers correspond to those given in Table 4.

of oxygen into the crucible. Thus, it appears that these impurities must in part be responsible for the observed ferrous iron reduction.

That substantial manganese accumulated in runs reported by Roeder (1974) is shown by a comparison of his original starting compositions with those of the run products (Roeder, personal communication, 1981). We find that polished sections of the

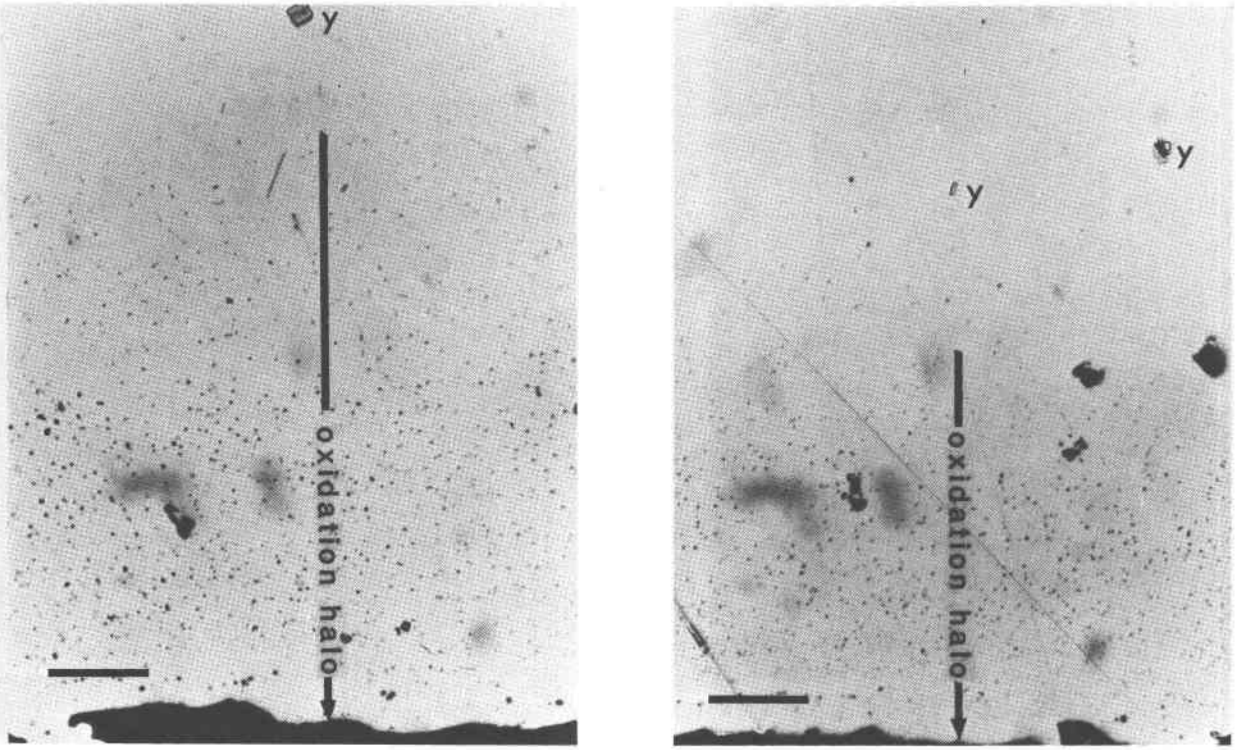

Fig. 4. Reflected-light photomicrographs (air) showing oxidation halo developed in H_2-treated electromagnet-grade iron crucibles containing charges and run for 8 hours (left) and 24 hours (right) (runs 10 and 6 in Table 4). The crucible–charge interface is at the bottom of each photograph. Bar scale represents 50 μm.

crucibles used by Roeder contain a substantial amount of manganese-rich inclusions (Table 1). We have also noted that in long runs at subsolidus temperatures, manganese-bearing capsules contaminate pyroxene by causing an anomalously high MnO content (as much as 5.5 wt.%) at the surface of originally manganese-poor (0.2% MnO) orthopyroxene plates.

Both FeO depletion and MnO and TiO_2 accumulation in silicate charges are alleviated by pretreating the electromagnet-grade crucibles in atmospheres more oxidizing than pure hydrogen (Figs. 5 and 6). Contamination of the charge by manganese and titanium and FeO loss was observed in runs using H_2-treated crucibles but was less notable in CO_2–H_2 treated crucibles. Increased concentration of manganese and titanium was barely detectable in charges contained in CO_2–CO-treated electromagnet-grade crucibles and FeO loss did not occur in runs of up to 68 hours duration. Minor FeO loss after heating for ~120 hours may have resulted from run times that exceeded those of crucible CO_2/CO pretreatment (this observation should be born in mind when making long runs in pretreated crucibles). Comparison of the CO_2–H_2 and the CO_2–CO results indicates that hydrogen occluded in the CO_2–H_2 treated crucibles may be partly responsible for bulk-composition changes of the charges, as previously suggested from the relative differences in crucible halo development as a function of pretreatment. Also, in runs using H_2-treated crucibles, minor devitrification of the inner wall of the silica tube is observed and may be attributed to the presence of minor H_2O generated through crucible–charge interaction. Pretreatment in CO_2–CO gas appears to affect immobilization of the manganese and titanium by converting these elements from the metallic state (in which they would diffuse rapidly) to oxides (which are relatively immobile in the iron). These observations are also consistent with results of open system experiments using electromagnet-grade iron by Schwerdtfeger and Muan (1966) using CO_2–CO gas mixtures and those of Roeder (1974) using CO_2–H_2 mixtures. Schwerdtfeger and Muan reported no appreciable gain of MnO or TiO_2 by Mn–Fe–Si–O compositions equili-

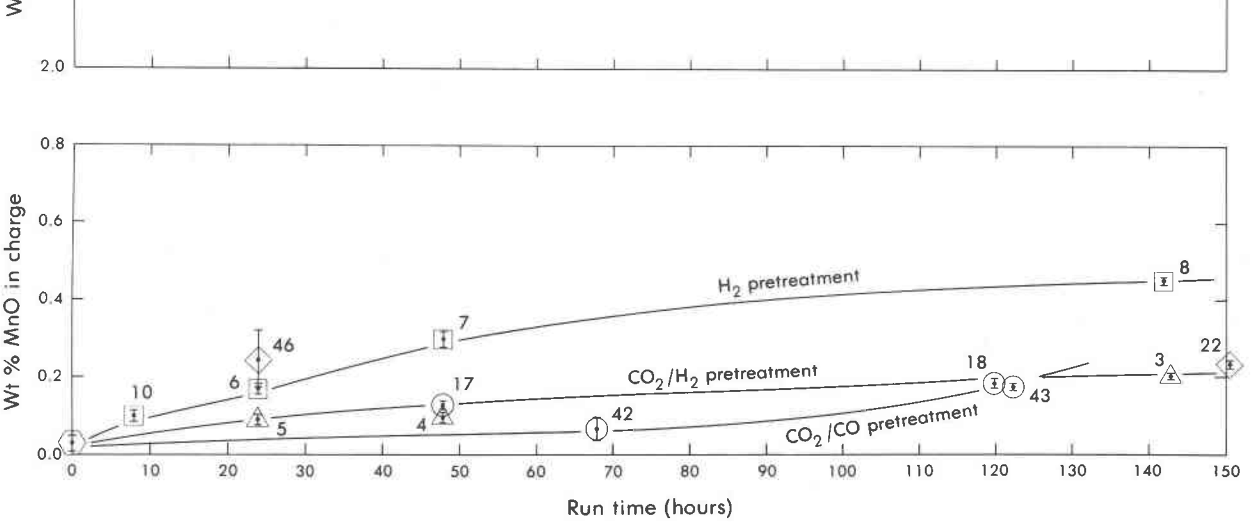

Fig. 5. Wt.% TiO_2 (above) and wt.% MnO (below) *vs.* time in charges run in electromagnet-grade iron crucibles pretreated in H_2 (squares), CO_2–H_2 (triangles), CO_2–CO (circles) and untreated (diamonds). The composition of the starting mixture (Table 3) is represented by a hexagon. Each point represents an average of three to five analyses and error bars define one standard deviation about the mean. Run numbers correspond to those in Table 4.

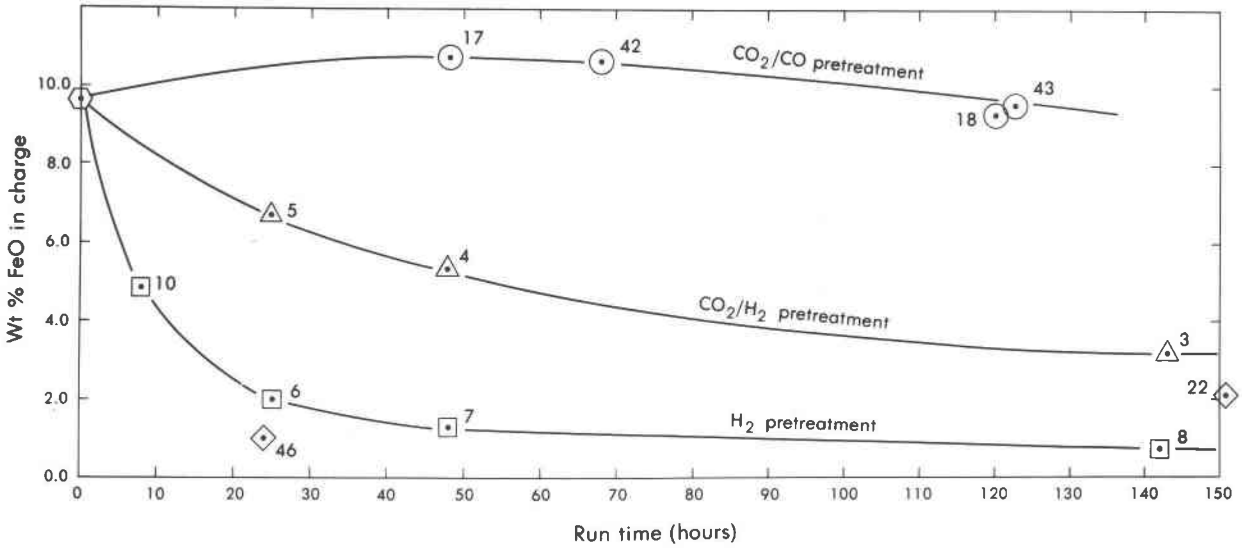

Fig. 6. Wt.% FeO *vs.* time in charges run in electromagnet-grade iron crucibles pretreated in H_2 (squares), CO_2–H_2 (triangles) and CO_2–CO (circles) and untreated (diamonds). The composition of the starting mixture (Table 3) is represented by a hexagon. Each point represents an average of three to five analyses and symbol size is considerably larger than one standard deviation about the mean for each data point. Run numbers correspond to those in Table 4.

brated in atmospheres of CO_2–CO whereas some manganese accumulation is evident in basaltic-melting experiments of Roeder (1974).

The lack of serious iron loss problems in experiments of Lipin and Muan (1975) and Lipin (1978) using electromagnet-grade iron crucibles in evacuated silica tubes could be explained by the intrinsic f_{O_2} of the specific lot of iron used. As shown in Figure 1b and Table 1, the "Lipin/Muan" material contains abundant elongate grey oxide blebs which appear to have a composition of mangano-wüstite. Crucibles of this material should have an intrinsic f_{O_2} relatively close to that of the silicate charge in equilibrium with metallic iron. Thus, there would be no tendency for substantial redox interaction between the charge and its container.

Conclusions

It is apparent that the ferrous oxide content of charges in iron crucibles varies in response to the local redox potential of the system. This redox potential can be defined by the f_{O_2} of the ambient atmosphere (in open systems), the incipient f_{O_2} of the starting material, and the f_{O_2} imposed by the iron crucible and its impurities. It is also dependent upon the temperature and duration of the run, as well as the presence of other components in the system which affect changes in the oxidation state of iron dependent of f_{O_2} (Thornber *et al.*, 1980; Roeder, 1974).

As suggested by previous investigators and as indicated by our results, high-purity iron crucibles can be used to contain iron-bearing silicate in closed systems without causing substantial bulk-composition changes. However, it is also apparent that the degree of charge–crucible redox interaction using impure iron crucibles can be highly variable. It appears that oxidation of crucible impurities is largely responsible for ferrous iron loss in iron-bearing oxide materials heated in impure iron crucibles and that the extent of iron-loss is dependent upon the intrinsic f_{O_2} of the crucible material as regulated by the nature of its impurities. The most prominent of the complement of reduction reactions, written to emphasize the direction of mass transfer, appear to be:

1. $Mn_{(crucible)} + FeO_{(charge)} \rightarrow MnO + Fe_{(charge+crucible)}$

2a. $Ti_{(crucible)} + 2FeO_{(charge)} \rightarrow TiO_2 + 2Fe_{(charge+crucible)}$

or

2b. $TiO_{(crucible)} + FeO_{(charge)} \rightarrow TiO_2 + Fe_{(charge+crucible)}$

3. $H_{2(crucible)} + FeO_{(charge)} \rightarrow Fe_{(charge)} + H_2O$

The technique for pretreatment of electromagnet-grade iron crucibles is a critical factor affecting subsequent redox equilibria in these experiments.

Results obtained using crucibles treated at 1050°C in atmospheres of variable hydrogen content suggest that the amount of occluded hydrogen affects the degree of exchange of the reducing impurities and oxygen between crucible and charge and is partly responsible for charge reduction. The rate and magnitude of interdiffusion of titanium, manganese, and oxygen between crucible and charge is dependent upon the f_{O_2} of capsule pretreatment and, to a lesser extent, the presence or absence of hydrogen in the system.

It appears that pretreatment of electromagnet-grade iron crucibles in CO_2–CO gas satisfactorily minimizes ferrous-iron loss by immobilizing the manganese and titanium impurities as oxide blebs (thereby hindering movement of manganese and/or titanium into the charge and of oxygen into the crucible) and by removing carbon (and hydrogen) present in untreated crucible material. Such a treatment may not be necessary for impure crucibles having an intrinsic f_{O_2} which is relatively close to the $Fe–Fe_{1-x}O$ buffer.

Acknowledgments

We want to thank Mary Woodruff for making many of the polished thin sections of the crucibles and James McGee for masterful maintenance of our moribund microprobe. Gordon L. Nord, Jr. provided the Mn analysis of the surface of the annealed pyroxene plate. Donald Lindsley (SUNY–Stony Brook) taught one of us (JSH) the usage of iron sponge. We appreciate the constructive reviews of this paper by David Walker (Harvard Univ), Ian Duncan (SMU), Peter Roeder (Queen's Univ) and I-Ming Chou and Bruce Lipin (U.S. Geol. Survey). This effort nucleated from a study of the crystallization of a lunar highlands fragmental basalt. We are grateful to the National Aeronautics and Space Administration for providing partial support through Contract T-781H.

References

Biggar, G. M., Humphries, D. J., and O'Hara, M. J. (1974) Experimental crystallization and geochemical interpretation of low titanium basalts. Lunar Science V, 60–62.

Bowen, N. L., and Schairer, J. F. (1932) The system $FeO–SiO_2$. American Journal of Science, 24, 177–213.

Bowen, N. L., Schairer, J. F. and Posnjak, E. (1933) The system, $CaO–FeO–SiO_2$. American Journal of Science, 26, 193–284.

Bowen, N. L. and Schairer, J. F. (1935) The system, $MgO–FeO–SiO_2$. American Journal of Science, 29, 151–217.

Green, D. H., Ringwood, A. E., Ware, N. G., and Hibberson, W. O. (1975) Experimental petrology and petrogenesis of Apollo 17 mare basalts (abstract). Lunar Science VI, 311–313.

Grove, T. L., Walker, D., Longhi, J., Stolper, E. and Hays, J. F. (1973) Petrology of rock 12002 and origin of picritic basalts at Oceanus Procellarum. Proceedings of the Lunar Science Conference 4th, 995–1011.

Huebner, J. S. (1975) Oxygen fugacity values of furnace gas mixtures. American Mineralogist, 60, 815–823.

Jarosewich, E., Nelen, J. A., and Norberg, J. A. (1979) Electron microprobe reference samples for mineral analyses. Smithsonian Contributions to the Earth Sciences no. 22 (R. F. Fudali, ed.) 68–72.

Kesson, S. E. (1975) Mare basalts: Melting experiments and petrogenetic interpretations. Proceedings of the Lunar Science Conference 6th, 921–944.

Lipin, B. R. and Muan, A. (1975) Equilibrium relations among iron–titanium oxides in silicate melts: The system $CaMgSi_2O_6$–"FeO"–TiO_2 in equilibrium with metallic iron. Proceedings of the Lunar Science Conference 6th, 945–958.

Lipin, B. R. (1978) The system $Mg_2SiO_4–Fe_2SiO_4–CaAl_2Si_2O_8–SiO_2$ and the origin of Fra Mauro basalts. American Mineralogist, 63, 350–364.

Longhi, J., Walker, D., Grove, T. L., Stolper, E. M., and Hays, J. F. (1974) The petrology of the Apollo 17 mare basalts. Proceedings of the Lunar Science Conference 5th, 447–469.

Muan, A. and Schairer, J. F. (1970) Melting relations of materials of lunar composition. Carnegie Institute of Washington Yearbook, 69, 243–245.

O'Hara, M. J. and Humphries, D. J. (1977) Problems of iron gain and loss during experimentation on natural rocks: the experimental crystallization of five lunar basalts at low pressures. Royal Society of London Philosophical Transactions, A 286, 313–330.

Roeder, P. L. (1974) Activity of iron and olivine solubility in basaltic liquids. Earth and Planetary Science Letters, 23, 397–410.

Schwerdtfeger, K. and Muan, A. (1966) Activities in olivine and pyroxenoid solid solution of the system Fe–Mn–Si–O at 1150°C. Metallurgical Society AIME Transactions, 236, 201–210.

Thornber, C. R., Roeder, P. L., and Foster, J. R. (1980) The effect of composition on the ferric–ferrous ratio in basaltic liquids at atmospheric pressure. Geochimica et Cosmochimica Acta, 44, 525–532.

Thornber, C. R. and Huebner, J. S. (1980) An experimental study of the thermal history of fragment-laden "basalt" 77115. Proceedings of the Conference of the Lunar Highlands Crust (J. J. Papike and R. B. Merrill, eds.) p. 233–252.

Walker, D., Longhi, J., and Hayes, J. F. (1972) Experimental petrology and origin of Fra Mauro rocks and soil. Proceedings of the Third Lunar Science Conference, 1, 797–817.

Walker, D., Longhi, J., Stolper, E. M., Grove, T. L. and Hays, J. F. (1975) Origin of titaniferous lunar basalts. Geochimica et Cosmochimica Acta, 39, 1219–1235.

Walker, D., Kirkpatrick, R. J., Longhi, J., and Hays, J. F. (1976) Crystallization history of lunar picritic basalt sample 12002: phase equilibria and cooling rate studies. Geological Society of America Bulletin, 87, 646–656.

Walker, D., Longhi, J., Lasaga, A. C., Stolper, E. M., Grove, T. L. and Hays, J. F. (1977) Slowly cooled microgabbros 15555 and 15065. Proceedings of the Lunar Science Conference, 8th, 1521–1547.

Wiggins, L. B. and Huebner, J. S. (1981) Combined X-ray wavelength and energy dispersive analysis to increase microprobe efficiency. U.S. Geological Survey Open File Report #81-1041.

Manuscript received, January 28, 1982;
accepted for publication, July 22, 1982.